Earth and Planetary Science Letters 410 (2015) 54–61

Contents lists available at ScienceDirect

Earth and Planetary Science Letters

www.elsevier.com/locate/epsl

Late formation of a comet Wild 2 crystalline silicate particle, Pyxie, inferred from Al–Mg chronology of plagioclase

Daisuke Nakashima [a,*,1], Takayuki Ushikubo [a,b], Noriko T. Kita [a], Michael K. Weisberg [c,d], Michael E. Zolensky [e], Denton S. Ebel [d]

[a] WiscSIMS, Department of Geoscience, University of Wisconsin-Madison, Madison, WI 53706, USA
[b] Kochi Institute for Core Sample Research, JAMSTEC, Monobe-otsu 200, Nankoku, Kochi 783-8502, Japan
[c] Department of Physical Sciences, Kingsborough College and Graduate Center of the City University of New York, 2001 Oriental Boulevard, Brooklyn, NY 11235, USA
[d] Department of Earth and Planetary Sciences, American Museum of Natural History, New York, NY 10024, USA
[e] Astromaterials Research and Exploration Science, NASA Johnson Space Center, Houston, TX 77058, USA

ARTICLE INFO

Article history:
Received 17 June 2014
Received in revised form 13 November 2014
Accepted 18 November 2014
Available online 5 December 2014
Editor: B. Marty

Keywords:
Al–Mg isotope systematics
crystalline silicate
comet 81P/Wild 2
solar system formation
Stardust

ABSTRACT

We examined the Al–Mg isotope systematics of plagioclase in a FeO-poor ferromagnesian Wild 2 particle (C2092,7,81,1,0; named Pyxie) using a ~2 μm spot. Three analyses show average $^{27}Al/^{24}Mg$ ratio of ~65 and excess $\delta^{26}Mg^*$ value of $+0.1 \pm 4.5‰$ (2σ), indicating no resolvable ^{26}Mg excess in the particle. The inferred initial $(^{26}Al/^{27}Al)_0$ ratio of plagioclase in Pyxie is estimated as $(-0.6 \pm 4.5) \times 10^{-6}$ with an upper limit of 4×10^{-6}. The result is very similar to that of the FeO-rich ferromagnesian particle "Iris" (Ogliore et al., 2012). Assuming homogeneous distribution of ^{26}Al in the early solar system, Pyxie formed at least 2.6 Ma after the oldest Ca–Al-rich inclusions. This minimum formation age is marginally younger than formation ages of most chondrules in type ~3.0 chondrites but comparable with those of Mg# < 98 chondrules in CR3 chondrites. Considered in conjunction with similar oxygen isotope ratios between Pyxie (and Iris) and Mg# < 98 chondrules in CR3 chondrites, it is inferred that the ferromagnesian Wild 2 particles and Mg# < 98 chondrules in CR3 chondrites formed late in local disk environments that had similar oxygen isotope ratios and redox states.

© 2014 Elsevier B.V. All rights reserved.

1. Introduction

Materials collected from comet Wild 2 contain abundant crystalline silicates, some of which resemble the Ca–Al-rich inclusions (CAIs) and chondrules in chondritic meteorites that probably formed at high temperatures (Brownlee et al., 2006; McKeegan et al., 2006; Zolensky et al., 2006; Nakamura et al., 2008, 2009; Simon et al., 2008; Ishii et al., 2008, 2009; Bridges et al., 2012; Joswiak et al., 2012; Ogliore et al., 2012). Organic material was also identified in Wild 2 particles, similar to the organics found in meteorites and chondritic interplanetary dust particles (IDPs) (Sandford et al., 2006; Sandford, 2008; Elsila et al., 2009; De Gregorio et al., 2011; Cody et al., 2011). Enrichments of deuterium and ^{15}N (McKeegan et al., 2006; Matrajt et al., 2008) in some of these Wild 2 particles indicate chemical reactions at low temperature in the interstellar medium or the early outer Solar System (Alexander et al., 2010). In addition, presolar grains have been identified from Wild 2 (McKeegan et al., 2006; Stadermann et al., 2008; Messenger et al., 2009) and their abundance is higher than those in meteorites and IDPs, though with large uncertainty (Leitner et al., 2010, 2012). It has been suggested that high temperature crystalline silicates were transported from the hot inner Solar System to the cold outer solar nebula regions, possibly due to radial diffusion in the protoplanetary disk (e.g., Ciesla, 2007, 2010, 2011; Hughes and Armitage, 2010).

Based on comparisons of chemistry, mineralogy, and oxygen isotope ratios of ferromagnesian Wild 2 particles with those of chondritic materials such as chondrules and matrix minerals, it was suggested that Wild 2 particles are related to carbonaceous chondrite chondrules (Nakamura et al., 2008) and materials in various types of chondrites (Joswiak et al., 2012; Frank et al., 2014). Nakashima et al. (2012) conducted a systematic survey of oxygen isotope ratios of ferromagnesian Wild 2 particles, and they compared $\Delta^{17}O$ ($= \delta^{17}O - 0.52 \times \delta^{18}O$) values and Mg# [= molar MgO/(MgO + FeO)%] of the Wild 2 particles with those of chondrules in known chondrite groups; $\Delta^{17}O$ and Mg# reflect

* Corresponding author. Tel./fax: +81 22 795 5903.
E-mail address: dnaka@m.tohoku.ac.jp (D. Nakashima).
[1] Present address: Department of Earth and Planetary Material Sciences, Faculty of Science, Tohoku University, Aoba, Sendai, Miyagi 980-8578, Japan.

http://dx.doi.org/10.1016/j.epsl.2014.11.020
0012-821X/© 2014 Elsevier B.V. All rights reserved.

oxygen isotope compositions and redox states of the reservoirs from which chondrules formed (Ushikubo et al., 2012). Similar to chondrules in carbonaceous chondrites (e.g., Connolly and Huss, 2010; Nakashima et al., 2010; Tenner et al., 2013a, 2014; Ushikubo et al., 2012; Schrader et al., 2013a, 2014), the ferromagnesian Wild 2 particles show a systematic trend wherein $\Delta^{17}O$ values increase with decreasing Mg#, which is most similar to that of chondrules in CR chondrites (Nakashima et al., 2012). Based on these similarities, Nakashima et al. (2012) inferred a link between ferromagnesian Wild 2 particles and chondrules in CR chondrites.

Chronology of early solar system materials, such as CAIs and chondrules, is very important for understanding the evolution of the protoplanetary disk (e.g., Kita et al., 2012, 2013) and radial transport of early-formed objects (e.g., Ciesla, 2010). While long-lived radiometric dating using the U–Pb system is considered to be the best means to determine accurate absolute formation time (Amelin et al., 2010; Connelly et al., 2012), however, Wild 2 particles are too small to apply this method (typically 10 μm in the longest diameter; e.g., Joswiak et al., 2012). Instead, relative chronometry using the ^{26}Al–^{26}Mg system is feasible because some Wild 2 particles contain minerals with high Al_2O_3 and low MgO, such as plagioclase and Al_2O_3-rich glass (Joswiak et al., 2012). The ^{26}Al–^{26}Mg system serves as a high time-resolution chronometer because of the short ^{26}Al half-life of 0.705 Myr (Norris et al., 1983). The secondary ion mass spectrometer (SIMS) has been proven to be very useful in the Al–Mg isotope analysis of $\leq$10 μm scale Al-rich phases in chondrules and CAIs from primitive chondrites (Kita et al., 2000, 2012; Kurahashi et al., 2008a; MacPherson et al., 2010, 2012; Makide et al., 2013; Ushikubo et al., 2013). Likewise, the SIMS Al–Mg isotope analyses of Wild 2 particles are important to understand their origin, though the analyses are technically challenging due to the small sample sizes ($\leq$10 μm). Previously, CAI-like particles Inti (track 25) and Coki (track 141) and the FeO-rich chondrule-like particle Iris (track 74) were analyzed for Al–Mg isotopes (Ishii et al., 2010; Matzel et al., 2010; Ogliore et al., 2012). The analyzed samples were TEM sections ($\sim$100 nm thick) that contained limited regions of Al-rich phases ($\leq$2 μm), which resulted in large analytical uncertainties (10–40‰ in 2SD for $\delta^{26}Mg^*$; Matzel et al., 2010; Ishii et al., 2010) or required special sample treatment (Pt deposition using FIB to cover Mg-rich phases; Ogliore et al., 2012). None of these particles showed resolvable excess of ^{26}Mg, showing upper limits of inferred initial $^{26}Al/^{27}Al$ from 3×10^{-6} (Ogliore et al., 2012) to 1×10^{-5} (Matzel et al., 2010), and suggesting late formation of the particles ($>$ few Ma after the oldest CAIs; Ishii et al., 2010; Matzel et al., 2010; Ogliore et al., 2012).

These CAI-like and FeO-rich chondrule-like Wild 2 particles are less abundant than FeO-poor ferromagnesian particles (Joswiak et al., 2012; Frank et al., 2014). Al–Mg isotope measurements of FeO-poor ferromagnesian particles have not been reported. Among nine ferromagnesian Wild 2 particles analyzed for oxygen three-isotope ratios by Nakashima et al. (2012), one particle, named "Pyxie", consists of FeO-poor low-Ca pyroxene and plagioclase with a large surface area ($\sim$10 μm), which is suitable for Al–Mg isotope analyses. This particle is embedded in epoxy resin (potted butt) with significant thickness, unlike the previously analyzed TEM sections. In this study, we present the results of SIMS Al–Mg isotope measurements of plagioclase in the FeO-poor ferromagnesian Wild 2 particle and address the origin of the particle.

2. Analytical procedures

2.1. Sample preparation

A terminal particle (C2092,7,81,1,0; nicknamed "Pyxie") extracted from Stardust track 81 was mounted in a 200 μm $\times$ 200 μm square top mesa of an 8 mm diameter epoxy cylinder. The top surface had been microtomed. To minimize surface topography that causes instrumental mass fractionation of measured isotope ratios using a SIMS (Kita et al., 2009), Pyxie's flat microtomed surface was embedded in epoxy resin along with a San Carlos olivine grain (running standard for oxygen isotope analyses; Nakashima et al., 2012), which was then ground and polished to a flat disk with a 8 mm radius and 2.5 mm thickness (Nakashima et al., 2012).

Because most of the plagioclase in Pyxie was underneath epoxy (Nakashima et al., 2012), the surface of Pyxie required further polishing to expose plagioclase for Al–Mg isotope analysis. Three-dimensional images of Pyxie were obtained using X-ray computed tomography (CT; a GE phoenix v|tome|x s240 μCT system) at American Museum of Natural History (cf., Friedrich et al., 2013) in order to estimate the remaining thickness of Pyxie and to minimize consumption of sample during the additional grinding. For X-ray CT observation, the X-ray energy was set to 60 keV, and pixel size was $\sim$1 μm. The thickness of Pyxie was estimated as $\sim$2 μm. Subsequently, the surface of Pyxie was ground carefully using a 0.25 μm diamond suspension until sufficient surface area of plagioclase was exposed for the SIMS Al–Mg isotope analysis. Since SIMS pits with depths of $\sim$1–2 μm remained from previous oxygen three-isotope analyses (Nakashima et al., 2012), the thickness that was removed during final polishing was less than 1 μm.

2.2. Electron microscopy

Major elemental compositions of Pyxie were measured using the CAMECA SX100 electron microprobe at the American Museum of Natural History equipped with five wavelength-dispersive X-ray spectrometers (WDS) before preparation of the 8 mm polished flat epoxy surface for oxygen isotope analyses (Nakashima et al., 2012). WDS quantitative chemical analyses of individual silicate phases were performed at 15 kV accelerating voltage and 20 nA beam current with a focused beam. Natural and synthetic standards were chosen based on the compositions of the minerals being analyzed (cf., Weisberg et al., 2011).

Backscattered electron (BSE) and secondary electron (SE) images of Pyxie were obtained using a field emission scanning electron microscope (FE-SEM; Zeiss LEO1530 at the University of Wisconsin) and a SEM (Hitachi S3400 at the University of Wisconsin) at several steps of sample preparation including after previous oxygen isotope analyses (Nakashima et al., 2012), after re-polishing, after FIB marking (see below), and after SIMS Al–Mg isotope analyses. Periods of exposure of samples to the electron beam were minimized so as to avoid significant depressions or deformation of epoxy surrounding Pyxie, because the topography or tilting of the sample surface could cause a significant instrumental mass fractionation in measured isotope ratios (Kita et al., 2009). After the Al–Mg isotope analyses, elemental compositions of plagioclase and low-Ca pyroxene in Pyxie were verified by semi-quantitative analyses using an energy-dispersive X-ray spectrometer (EDS).

2.3. FIB marking for sample aiming

For SIMS Al–Mg isotope analyses of Al-rich phases, overlapping analysis areas with adjacent Mg-rich phases, such as olivine and pyroxene, would result in several analytical problems, including lower $^{27}Al/^{24}Mg$ ratios and reduction of excess ^{26}Mg, inaccurate instrumental bias corrections, and potential artifacts from the quasi-simultaneous arrival (QSA) effect (Slodzian et al., 2004). To avoid hitting adjacent low-Ca pyroxene, we employed FIB (focused ion beam) marking at the selected locations of Pyxie prior to the SIMS analyses, with procedures similar to those described for oxygen isotope analyses of Wild 2 particles (Fig. 1; Nakashima et al., 2012). A Zeiss 1500XB CrossBeam workstation equipped with

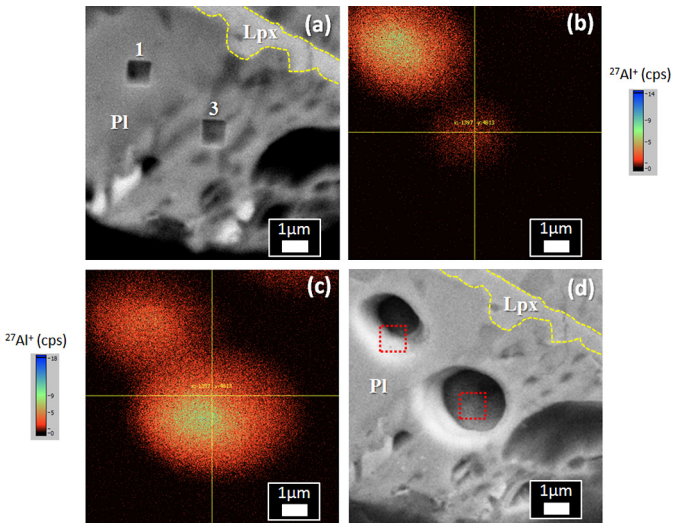

Fig. 1. A BSE image of Pyxie (terminal particle from track 81) after FIB marking (a), an $^{27}Al^+$ ion image (10 μm × 10 μm) of Pyxie showing the 1st-analyzed spot for Al–Mg isotopes (upper left) and a FIB mark before the 3rd spot analysis (center) (b), an $^{27}Al^+$ ion image (10 μm × 10 μm) of Pyxie after the 3rd spot analysis for Al–Mg isotopes (c), and a BSE image (using FE-SEM) of Pyxie after the Al–Mg isotope analyses (d). Numbers near the FIB marks in panel a indicate spot numbers of SIMS analysis, which correspond to spot numbers in Fig. 2 and Table 2. In panels a and d, irregular surface with many dimples of Pyxie was made by microtoming to obtain TEM thin sections, and dashed lines correspond to boundary between plagioclase (Pl) and low-Ca pyroxene (Lpx). In panels b and c, centers of cross-wires correspond to the center of the O^- primary beam. The $^{27}Al^+$ ion images were taken in 512 × 512 pixels (~20 nm/pixel) and in linear scale. In panel d, outline of the two FIB squares (dotted lines) in panel a is overlaid.

a gallium ion source at the University of Wisconsin was used to remove surface carbon coating (~20 nm thick) from Pyxie and an anorthitic glass standard (see the Supplementary information). A 30 keV focused Ga^+ ion beam set to 5 pA was rastered within a 1 μm × 1 μm square on the sample surface for 120 s, so that only the surface coating was removed without significant milling of underlying silicate mineral (Fig. 1a). This 1 μm square region was later identified by secondary $^{27}Al^+$ ion imaging in SIMS before Al–Mg isotope analysis.

2.4. Al–Mg isotope analysis

Magnesium isotope ratios and $^{27}Al/^{24}Mg$ ratios of plagioclase in Pyxie were analyzed with the CAMECA IMS-1280 at WiscSIMS. The analytical conditions and measurement procedures were generally similar to those in Ushikubo et al. (2013), otherwise described below. The 8 mm epoxy disk containing Pyxie was mounted in the sample holding disk (25 mm in diameter) with three holes (8 mm in diameter), which minimized the surface topography effects on high precision SIMS stable isotope analyses of cometary particles (Nakashima et al., 2011a). Prior to each Al–Mg isotope analysis, secondary $^{27}Al^+$ ion images of FIB squares were obtained using an O^- ion beam of ~2 μm diameter (~3 pA) that was rastered over an area of 10 μm × 10 μm. The primary beam was set as Köhler illumination mode with mass and beam apertures of 20 μm and 100 μm diameter. The secondary $^{27}Al^+$ ions were produced only from FIB squares where surface coating was removed and were detected as scanning ion images (Fig. 1b) using a fixed position mono-collector electron multiplier (mono-EM) at the ion optical axis. After the recognition of the FIB square (within a few minute sputtering), we moved the stage in order to relocate the FIB square to the center of the 10 μm × 10 μm raster area where the Al–Mg isotope analysis was made. New 10 μm × 10 μm $^{27}Al^+$ ion images were taken after each SIMS analysis to confirm the positions of analyzed spots (Fig. 1c).

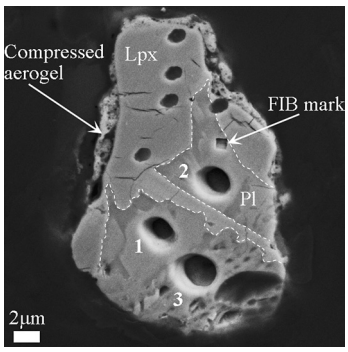

Fig. 2. A BSE image of Pyxie after Al–Mg isotope analyses. Numbers near the SIMS pits indicate spot numbers of SIMS analysis, which correspond to spot numbers in Table 2. Dashed lines correspond to boundary between plagioclase (Pl) and low-Ca pyroxene (Lpx). Five small holes in low-Ca pyroxene are SIMS pits for oxygen isotope analyses (Nakashima et al., 2012).

For Al–Mg isotope analysis, an O^- primary beam was set to ~2 μm and intensity of ~3 pA without raster. The secondary $^{24}Mg^+$, $^{25}Mg^+$, $^{26}Mg^+$, and $^{27}Al^+$ ions were detected using the mono-EM in magnet peak switching mode. Intensities of $^{24}Mg^+$ and $^{27}Al^+$ were $(1-2)\times10^3$ cps and $(0.6-1.3)\times10^5$ cps, respectively. Each spot analysis took ~11 hours, including 900 s of presputtering to stabilize Mg ion intensity, ~60 s for automatic centering of the secondary optics, and 600 cycles of switching between $^{24}Mg^+$, $^{25}Mg^+$, $^{26}Mg^+$, and $^{27}Al^+$ (counting times of 5, 20, 20, and 1 s, respectively, with 2 s waiting time). Individual SIMS pits were carefully examined for cracks and overlapping phases using FE-SEM (Fig. 1d).

An isotope mass fractionation correction (both instrumental and natural) was applied to the SIMS-measured Mg isotope ratios in order to estimate excess ^{26}Mg (Kita et al., 2012). The terrestrial Mg isotope ratios of $(^{25}Mg/^{24}Mg) = 0.12663$ and $(^{26}Mg/^{24}Mg) = 0.13932$ (Catanzaro et al., 1966) are used for data reduction of the measured Mg isotope ratios. The fractionation-corrected $\delta^{26}Mg^*$ values were calculated using an exponential law with the coefficient $\beta = 0.514$ (Davis et al., 2005) from the evaporation experiments of Richter et al. (2007).

We analyzed a synthetic anorthitic glass standard with MgO of 0.6 wt% ($Al_2O_3/MgO = 72.25$; Kita et al., 2012) before and after unknown sample analyses. Reproducibility of $\delta^{26}Mg^*$ values of this standard was better than 1‰, though showing a small positive bias from +1.0‰ to +2.5‰ with uncertainty of $\sim\pm3$‰ (2SE). The average value of the $\delta^{26}Mg^*$ bias (+1.7 ± 1.1‰; 2SD; $n = 5$) was corrected for unknown samples (see the Supplementary information). The 2SE ($= 2SD/\sqrt{(n)}$) of the average $\delta^{26}Mg^*$ value of the anorthitic glass standard was propagated as an uncertainty to those of $\delta^{26}Mg^*$ values of individual spot analyses. A relative sensitivity factor, RSF $= (^{27}Al/^{24}Mg)_{SIMS}/(^{27}Al/^{24}Mg)_{EPMA}$, was estimated using the anorthitic glass standard. The reproducibility of $^{27}Al/^{24}Mg$ ratios of the standard was 5% (2SD), which is propagated as an uncertainty to those of $^{27}Al/^{24}Mg$ ratios of individual spot analyses.

3. Sample description

Pyxie, which is "F1/T81" in Nakashima et al. (2012), is the terminal particle (~15 × 20 μm; Fig. 2) from track 81 (see http://www.curator.jsc.nasa.gov/stardust/catalog/index.cfm) and is surrounded by compressed aerogel. The major mineral phases of Pyxie are FeO-poor low-Ca pyroxene ($En_{92}Wo_3$; ~5 μm × 10 μm) and plagioclase ($An_{65}Ab_{35}$; ~10 μm × 10 μm; Table 1), which is consistent with the observation that a TEM section of the particle is a polycrystalline aggregate of low-Ca pyroxene and plagioclase (Dobrică and Brearley, 2011).

Table 1
Major elemental compositions (wt%) of Low-Ca pyroxene and plagioclase in Pyxie (C2092,7,81,1,0) obtained by electron microprobe analyses.

	Lpx	Pl
SiO_2	56.1	58.0
TiO_2	0.2	bd
Al_2O_3	1.1	22.5
Cr_2O_3	1.0	bd
FeO	3.2	0.5
MnO	0.8	bd
MgO	32.9	0.4
CaO	1.3	10.4
Na_2O	bd	3.1
K_2O	bd	bd
NiO	bd	bd
Total	96.6	94.9
En	92	
Wo	3	
An		65
Ab		35

bd = below detection limit.

Table 2
The Al–Mg isotope analyses of plagioclase in Pyxie (C2092,7,81,1,0).

Spot #	$^{27}Al/^{24}Mg \pm 2\sigma$		$\delta^{26}Mg^* \pm 2\sigma$ (‰)	
1	65.4	3.9	0.9	4.6
2	64.4	3.8	1.9	3.7
3	63.8	3.8	−2.4	3.1

Oxygen isotope ratios of low-Ca pyroxene in Pyxie were reproducible within analytical uncertainties (Nakashima et al., 2012). The average and 2SE of $\Delta^{17}O$ values were -1.1 ± 0.8‰ ($n = 5$), which is similar to those of FeO-poor ferromagnesian Wild 2 particles ($\Delta^{17}O$ from −3.0‰ to −1.9‰; Nakamura et al., 2008; Nakashima et al., 2011b, 2012).

4. Results

4.1. Mineralogy and chemistry of Pyxie

After repolishing, we recognized that a pyroxene lath with a width of 1–2 μm occurs in the plagioclase domain (Fig. 2) and is slightly enriched in Ca and Al compared to the large low-Ca pyroxene grain (detected by SEM-EDS). This is consistent with the observation of Ca-bearing pyroxene along with low-Ca pyroxene and plagioclase in a TEM section of the same particle (Dobrică and Brearley, 2011). Low-Ca pyroxene in Pyxie contains 1.0 wt% Cr_2O_3 and 0.8 wt% MnO (Table 1), similar to those observed in low-Ca pyroxene in the TEM section, but the Al_2O_3 content in Pyxie low-Ca pyroxene (1.1 wt%) is lower than that determined in the TEM section (~2.6 wt%; Dobrică and Brearley, 2011). Plagioclase in Pyxie contains 0.4 wt% MgO, and K_2O was below detection limits of EPMA (Table 1) and SEM-EDS.

4.2. Results of Al–Mg isotope analyses

We made three spot analyses in plagioclase of Pyxie (Fig. 2), which are summarized in Table 2. A complete data table including standard analyses is given in the Supplementary Table A1. Sizes of the SIMS pits for Al–Mg isotope analyses became slightly larger for spots 2 and 3 than spot 1 because internal diameter of the 20 μm aperture in primary ion column was enlarged during the analysis session as it was sputtered by intense O^- primary ions (Fig. 2). However, the spot sizes remained within 3 μm until the end of sample analysis and did not overlap low-Ca pyroxene nor surrounding epoxy and aerogel.

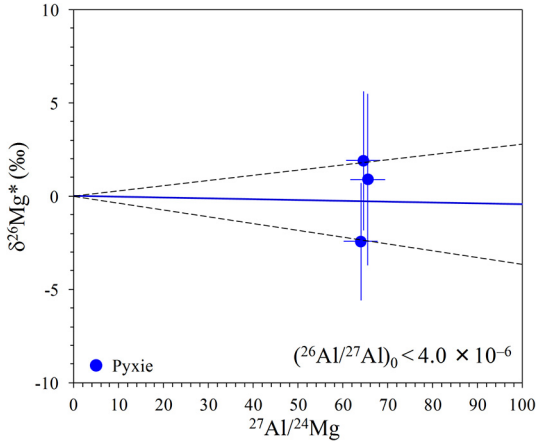

Fig. 3. Al–Mg isochron diagram of Pyxie. Errors are 2σ. Dashed lines represent 2σ confidence lines for the regression line (solid line, blue in the web version).

Plagioclase in Pyxie shows $^{27}Al/^{24}Mg$ ratios ranging from 64 to 65 (Fig. 3), which is generally consistent with EPMA analyses (Table 1) and similar to those of plagioclase in chondrules in type ~3.0 chondrites (typically <100; Kita and Ushikubo, 2012). The $\delta^{26}Mg^*$ values of three analyses range from −2‰ to +2‰ with uncertainty of ~ ±4‰ (2SE) (Fig. 3), indicating that there is no resolvable excess in ^{26}Mg. A regression of the data forcing to the origin using ISOPLOT (York fit program; Ludwig, 2003) yields an (model) isochron with a slope of $-0.004 \pm 0.032(2\sigma)$ on the $^{27}Al/^{24}Mg$ versus $\delta^{26}Mg^*$(‰) diagram (Fig. 3). The inferred initial $^{26}Al/^{27}Al$ ratio, $(^{26}Al/^{27}Al)_0$, of plagioclase in Pyxie is estimated as $(-0.6 \pm 4.5) \times 10^{-6}$ (2σ) with a one-sided upper limit of 4.0×10^{-6}.

5. Discussion

5.1. Initial ^{26}Al abundance at the time of crystallization of Pyxie

Plagioclase in Pyxie shows no resolvable excess ^{26}Mg, with a 2σ upper limit of 4.0×10^{-6} for $(^{26}Al/^{27}Al)_0$ (Fig. 3), which is attributed to either low abundance of ^{26}Al at the time of crystallization or loss of radiogenic ^{26}Mg by later disturbance. The effect of thermal metamorphism to the Al–Mg system cannot be totally ruled out as the majority of Wild 2 olivine has reportedly been slightly metamorphosed similar to petrographic subtypes up to 3.05–3.15 (Frank et al., 2014). Indeed, An# (65) and MgO content (0.4 wt%) of the plagioclase in Pyxie are lower than those of type I chondrules in type 3.0 chondrites, but similar to those in petrologic types >3.1 (Tenner et al., 2014b). However, we did not observe either nepheline or sodalite in Pyxie, which often accompanies loss of radiogenic ^{26}Mg (e.g., Maruyama and Yurimoto, 2003; Kita et al., 2004). The concentrations of K and Cl in Pyxie plagioclase were below detection limits of EPMA (Table 1) and SEM-EDS. The presence of rare cubanite (Cu-bearing iron sulfide; Berger et al., 2011) and Mg-carbonate (Mikouchi et al., 2007) in Wild 2 particles constrains the upper limit of the temperature of comet Wild 2 (<210 °C; Berger et al., 2011). Diffusion of Mg in plagioclase of An_{65} is very limited (≪1 nm; Van Orman et al., 2014) under such low temperature conditions even for 4.5 Gyr. Disturbance of the Al–Mg isotopic system during capture in aerogel ($T \leq 2000$ K, $t < 1$ μs; Brownlee et al., 2006) is unlikely because Mg diffusion in plagioclase of An_{65} is less than 1 nm (Van Orman et al., 2014). Thus, we suggest that the ^{26}Al abundance was low at the time and place of crystallization of Pyxie, similar to the case of other Wild 2 particles (Ishii et al., 2010; Matzel et al., 2010; Ogliore et al., 2012). Assuming homogeneous distribution of ^{26}Al in the early solar system, the 2σ upper limit of 4.0×10^{-6} for

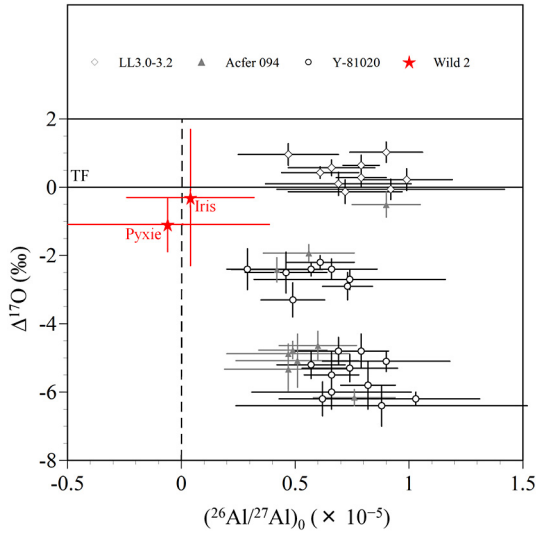

Fig. 4. A comparison between $(^{26}Al/^{27}Al)_0$ ratios and $\Delta^{17}O$ values of ferromagnesian Wild 2 particles, chondrules from LL3.0-3.2, Acfer 094, and CO3.0 (Yamato-81020) chondrites. The chondrule data from a CO3.0 chondrite consist of both type I and type II chondrules but those from Acfer 094 and LL3 chondrites consist only of type I chondrules and mainly of type II chondrules, respectively. Literature data of the Wild 2 particles are from Nakashima et al. (2012) and Ogliore et al. (2012). The $(^{26}Al/^{27}Al)_0$ ratios and $\Delta^{17}O$ values of chondrules are from Kita et al. (2000, 2010), Kurahashi et al. (2008a), Ushikubo et al. (2012, 2013), Tenner et al. (2013a). Errors are 2σ.

$(^{26}Al/^{27}Al)_0$ indicates that crystallization of Pyxie postdated the formation of the oldest CAIs ($(^{26}Al/^{27}Al)_0 = 5.25 \times 10^{-5}$; Larsen et al., 2011) by at least 2.6 Ma.

5.2. Comparison to $(^{26}Al/^{27}Al)_0$ ratios of chondrules and link to CR chondrites

Pyxie is one of the ferromagnesian Wild 2 particles analyzed for oxygen isotope ratios and classified into a FeO-poor group with $\Delta^{17}O$ values of ~ -2‰ in Nakashima et al. (2012). Along with the FeO-rich Wild 2 particle group of which $\Delta^{17}O$ values mainly range from ~ -2‰ to $+2$‰, the FeO-poor group was compared with chondrules in primitive (≤3.0) chondrites (see Introduction). The $\Delta^{17}O$–Mg# trend of the ferromagnesian Wild 2 particles is most similar to that of chondrules in CR chondrites (Connolly and Huss, 2010; Tenner et al., in press; Schrader et al., 2013a). Based on this similarity, Nakashima et al. (2012) inferred a link between ferromagnesian Wild 2 particles including Pyxie and chondrules in CR chondrites. It is not obvious from the texture if Pyxie is a chondrule fragment (Fig. 2) unlike the chondrule-like Wild 2 particles that exhibit igneous (e.g., porphyritic with glassy mesostasis) texture (Nakamura et al., 2008; Ogliore et al., 2012). However, the non-porous texture and enrichment of Cr_2O_3 and Al_2O_3 in the low-Ca pyroxene in Pyxie is characteristic for igneous pyroxene (Campbell and Borley, 1974; Dobrică and Brearley, 2011). Furthermore, the MgO content in Pyxie plagioclase (0.4 wt%; Table 1) is within the range of MgO contents in chondrule plagioclase in primitive chondrites (Tenner et al., 2014b) but higher than those in plagioclase in achondrites (Mittlefehldt et al., 1998). Thus, the mineral chemistry of Pyxie is consistent with an igneous origin (characteristics of chondrules). Here we further compare ferromagnesian Wild 2 particles and chondrules based on $(^{26}Al/^{27}Al)_0$ ratios, $\Delta^{17}O$ values, and Mg#.

In Fig. 4, we plot $\Delta^{17}O$ values of ferromagnesian Wild 2 particles (including the type-II chondrule fragment, Iris from Ogliore et al., 2012) against their $(^{26}Al/^{27}Al)_0$ ratios along with chondrules from LL3, CO3.0, and Acfer 094 (ungrouped 3.0) chondrites with recent high precision oxygen and Al–Mg isotope data (Kita et al., 2000, 2010; Kurahashi et al., 2008a; Ushikubo et al., 2012, 2013; Tenner et al., 2013a). Two ferromagnesian Wild 2 particles do not show resolvable excess ^{26}Mg; Pyxie with a $\Delta^{17}O$ value of ~ -1.1‰ and Mg# of 95 and Iris with $\Delta^{17}O$ of ~ -0.3‰ and Mg# of 64 (Fig. 4). In LL3, CO3.0, and Acfer 094 chondrites, chondrules consistently show resolvable ^{26}Mg excesses with similar $(^{26}Al/^{27}Al)_0$ ratios of $(0.2–1.0) \times 10^{-5}$, regardless of Mg# and $\Delta^{17}O$ (Kita et al., 2010; Ushikubo et al., 2013; Tenner et al., 2013a). In contrast, many chondrules in CR chondrites show $(^{26}Al/^{27}Al)_0$ ratios that are lower than 3×10^{-6} (>3 Ma after CAIs), most of which do not show resolvable ^{26}Mg excess in plagioclase (Nagashima et al., 2007, 2008; Kurahashi et al., 2008b; Hutcheon et al., 2009; Schrader et al., 2013b). Recently, Tenner et al. (2013b) revealed that the $\Delta^{17}O$ and Mg# trend of chondrules in CR3.0 chondrites relates to their ^{26}Al–^{26}Mg chronology; chondrules with $\Delta^{17}O$ values of > -3‰ and Mg# < 98 do not show resolvable ^{26}Mg excess with 2σ upper limits of $(^{26}Al/^{27}Al)_0$ ratio of 3×10^{-6}, while those with $\Delta^{17}O$ values of ~ -5‰ and Mg# > 98 show resolvable ^{26}Mg excess and a $(^{26}Al/^{27}Al)_0$ ratio of $\sim 5 \times 10^{-6}$. The two ferromagnesian Wild 2 particles (Fig. 4) are most similar to the subset of chondrules in CR3.0 chondrites with $\Delta^{17}O > -3$‰ and $(^{26}Al/^{27}Al)_0$ ratios $< 3 \times 10^{-6}$.

As mentioned earlier, the correlation between $\Delta^{17}O$ and Mg# in Wild 2 minerals most resembles that of chondrules in CR chondrites (Nakashima et al., 2012). Based on this relationship, we suggested a link between the ferromagnesian Wild 2 particles and chondrules in CR chondrites. However, we also argued that they are not identical because Wild 2 particles contain more FeO-rich phases while chondrules in CR3 chondrites are predominantly FeO-poor type I chondrules (Dobrică et al., 2009; Tenner et al., in press; Frank et al., 2014), suggesting that ferromagnesian particles which formed in an oxidizing environment were abundant where trans-Neptunian objects accreted. The chemistry of Pyxie and Iris is different from that in chondrules in CR3 chondrites. The plagioclase in Pyxie (An_{65}) is more Na-rich than that observed in type I chondrules in CR3 chondrites ($An_{80–99}$; Tenner et al., 2014b). The Iris mesostasis is Fe-poor and Na-rich compared to mesostasis in type II (FeO-rich; Mg# < 90) CR chondrules, and the Iris olivine is Ca- and Al-rich relative to olivine in type II CR chondrules (Ogliore et al., 2012). In spite of these differences, similarities of $\Delta^{17}O$, Mg#, and the low abundance of ^{26}Al of ferromagnesian Wild 2 particles and CR chondrite chondrules with $\Delta^{17}O > -3$‰ suggest that they formed late in local disk environments that had similar oxygen isotope ratios and redox states. As discussed in Nakashima et al. (2012), isotope anomalies of hydrogen and nitrogen in CR chondrites are attributed to low-temperature chemical reactions in the interstellar medium or the early outer solar system (Weisberg et al., 1995; Busemann et al., 2006; Floss and Stadermann, 2009; Alexander et al., 2010), the environments in which the Wild 2 particles and younger generations of CR chondrite chondrules formed could be the regions of chondrule formation farthest from the sun.

5.3. Low abundance of ^{26}Al in Wild 2 particles: implication for their origin

Both Ca–Al-rich and ferromagnesian Wild 2 particles analyzed for Al–Mg isotopes consistently show no resolvable excesses in ^{26}Mg (Ishii et al., 2010; Matzel et al., 2010; Ogliore et al., 2012; this study). The two particles Inti and Coki show refractory-rich mineralogies with ^{16}O-rich oxygen isotope signatures ($\Delta^{17}O \sim -20$‰) similar to CAIs in primitive chondrites (McKeegan et al., 2006; Simon et al., 2008; Ishii et al., 2009). The upper limits of inferred $(^{26}Al/^{27}Al)_0$ ratios (1×10^{-5} at 2σ for Coki) are significantly lower than "canonical" CAIs, typically $(4–5) \times 10^{-5}$ (Kita et al., 2013, references therein). The lack of resolvable excesses of ^{26}Mg could also be attributed to particle formation prior to

injection and homogenization of ^{26}Al in the protoplanetary disk, as is hypothesized for highly refractory phases (corundum and hibonite) and FUN (Fractionation and Unknown Nuclear effects) CAIs with no ^{26}Mg excess (e.g., Sahijpal and Goswami, 1998; Krot et al., 2012). However, late formation is preferred for explaining the CAI-like Wild 2 objects, because of their distinct mineralogy composed of anorthite, pyroxene, and spinel (Ishii et al., 2010; Matzel et al., 2010) and lack of significant mass dependent fractionation of the oxygen isotope ratios, unlike fractionated CAIs with nucleosynthetic anomalies of unknown origin ("FUN"; McKeegan et al., 2006). While the refractory compositions of the two CAI-like particles are consistent with their formation in a gas of Solar composition (Beckett et al., 1988), Mg# $<$ 95 for the two ferromagnesian Wild 2 particles Pyxie and Iris must be explained by their formation in an oxidizing environment, such as one with CI dust enrichment exceeding 200$\times$ (Ebel and Grossman, 2000). It is unlikely that such a dust-enriched environment existed before the ^{26}Al injection which may have simultaneously occurred with collapse of the Solar molecular cloud due to a supernova shock (Boss and Keiser, 2012). Thus, we infer that the Wild 2 particles with no clear evidence of extinct ^{26}Al could represent younger generations of high temperature solids ($>$ few Ma after CAIs) that formed in places with regionally heterogeneous oxygen isotope compositions and redox states. Astrophysical models (e.g., Ciesla, 2007; Hughes and Armitage, 2010) suggest that place was the inner solar nebula and that these particles were then radially transported to outer solar nebula regions ($\sim$35 AU; Duncan and Levison, 1997) where they accreted with ice to form comet Wild 2.

6. Conclusions

We performed Al–Mg isotope measurements of plagioclase in a FeO-poor ferromagnesian Wild 2 particle (Pyxie) using a $\sim$2 μm spot. The ^{27}Al/^{24}Mg ratios are $\sim$65, and δ^{26}Mg* values are from -2‰ to $+2$‰ with uncertainty of ± 4‰ (2SE), indicating no excess of ^{26}Mg derived from extinct ^{26}Al. The initial $(^{26}\mathrm{Al}/^{27}\mathrm{Al})_0$ ratio of plagioclase in Pyxie is estimated as $(-0.6 \pm 4.5) \times 10^{-6}$, (2σ) and the inferred upper limit is 4.0×10^{-6}. Since there is no clear evidence for loss of radiogenic ^{26}Mg by later disturbance of plagioclase in Pyxie, it is suggested that plagioclase in Pyxie crystallized under a low abundance of extinct ^{26}Al, probably indicating late formation. Assuming homogeneous distribution of ^{26}Al in the early solar system, crystallization of Pyxie postdated formation of excess ^{26}Mg-rich CAIs by at least 2.6 Ma. This formation age is also younger than those of most chondrules but comparable with those of Mg# $<$ 98 chondrules in CR3 chondrites (Tenner et al., 2013b). Considered in conjunction with similar Δ^{17}O values between Pyxie (and Iris) and Mg# $<$ 98 chondrules in CR3 chondrites (Nakashima et al., 2012), we infer that the ferromagnesian Wild 2 particles and Mg# $<$ 98 chondrules in CR3 chondrites formed late in local disk environments that had similar oxygen isotope ratios and redox states, which could be the radially furthest regions of chondrule formation (cf., Nakashima et al., 2012).

Wild 2 particles that have been analyzed for Al–Mg isotopes consistently show no resolvable excess of ^{26}Mg, regardless of distinct chemistries (refractory-rich and FeO-poor and –rich ferromagnesian) and variable Δ^{17}O values from ~ -20‰ to 0‰, which reflect formation environments (McKeegan et al., 2006; Simon et al., 2008; Ishii et al., 2009, 2010; Matzel et al., 2010; Nakashima et al., 2012; Ogliore et al., 2012; this study). These Wild 2 particles could represent younger generations of high temperature solids ($>$ few Ma after CAIs) that formed where oxygen isotope compositions and redox states were regionally heterogeneous.

Acknowledgements

Two anonymous reviewers provided helpful comments that improved this manuscript. The authors thank R.K. Noll for help with FIB and FE-SEM observation, J. Thostenson (American Museum of Natural History) for X-ray CT support, J. Kern for SIMS support, T.J. Tenner for discussion, and R.C. Ogliore (University of Hawai'i) for kindly providing the Al–Mg isotope data of the Wild 2 particle Iris. The Zeiss 1500XB CrossBeam workstation at the University of Wisconsin is supported by the UW MRSEC (DMR-1121288) and the UW NSEC (DMR-0832760). This work was supported by NASA (NK: NNX09AC30G, NNX13AD15G; DSE: NNX10AI42G; MKW: NNX12AI06G; Cosmochemistry for MEZ). WiscSIMS is partly supported by NSF-EAR (0319230, 0744079, 1053466).

Appendix A. Supplementary material

Supplementary material related to this article can be found online at http://dx.doi.org/10.1016/j.epsl.2014.11.020.

References

Alexander, C.M.O'D., Newsome, S.D., Fogel, M.L., Nittler, L.R., Busemann, H., Cody, G.D., 2010. Deuterium enrichments in chondritic macromolecular material-Implications for the origin and evolution of organics, water and asteroids. Geochim. Cosmochim. Acta 74, 4417–4437.

Amelin, Y., Kaltenbach, A., Iizuka, T., Stirling, C.H., Ireland, T.R., Petaev, M., Jacobsen, S.B., 2010. U–Pb chronology of the Solar System's oldest solids with variable ^{238}U/^{235}U. Earth Planet. Sci. Lett. 300, 343–350.

Beckett, J.R., Live, D., Tsay, F.-D., Grossman, L., Stolper, E., 1988. Ti^{3+} in meteoritic and synthetic hibonite. Geochim. Cosmochim. Acta 52, 1479–1495.

Berger, E.L., Zega, T.J., Keller, L.P., Lauretta, D.S., 2011. Evidence for aqueous activity on comet 81P/Wild 2 from sulfide mineral assemblages in Stardust samples and CI chondrites. Geochim. Cosmochim. Acta 75, 3501–3513.

Boss, A.P., Keiser, S.A., 2012. Supernova-triggered molecular cloud collapse and the Rayleigh–Taylor fingers that polluted the solar nebula. Astrophys. J. Lett. 756, L9.

Bridges, J.C., Changela, H.G., Nayakshin, S., Starkey, N.A., Franchi, I.A., 2012. Chondrule fragments from Comet Wild 2: evidence for high temperature processing in the outer Solar System. Earth Planet. Sci. Lett. 341–344, 186–194.

Brownlee, D., Tsou, P., Aleon, J., Alexander, C.M.O., Araki, T., Bajt, S., Baratta, G.A., Bastien, R., Bland, P., Bleuet, P., Borg, J., Bradley, J.P., Brearley, A., Brenker, F., Brennan, S., Bridges, J.C., Browning, N.D., Brucato, J.R., Bullock, E., Burchell, M.J., Busemann, H., Butterworth, A., Chaussidon, M., Cheuvront, A., Chi, M., Cintala, M.J., Clark, B.C., Clemett, S.J., Cody, G., Colangeli, L., Cooper, G., Cordier, P., Daghlian, C., Dai, Z., D'hendecourt, L., Djouadi, Z., Dominguez, G., Duxbury, T., Dworkin, J.P., Ebel, D.S., Economou, T.E., Fakra, S., Fairey, S.A.J., Fallon, S., Ferrini, G., Ferroir, T., Fleckenstein, H., Floss, C., Flynn, G., Franchi, I.A., Fries, M., Gainsforth, Z., Gallien, J.-P., Genge, M., Gilles, M.K., Gillet, P., Gilmour, J., Glavin, D.P., Gounelle, M., Grady, M.M., Graham, G.A., Grant, P.G., Green, S.F., Grossemy, F., Grossman, L., Grossman, J.N., Guan, Y., Hagiya, K., Harvey, R., Heck, P., Herzog, G.F., Hoppe, P., Horz, F., Huth, J., Hutcheon, I.D., Ignatyev, K., Ishii, H., Ito, M., Jacob, D., Jacobsen, C., Jacobsen, S., Jones, S., Joswiak, D., Jurewicz, A., Kearsley, A.T., Keller, L.P., Khodja, H., Kilcoyne, A.D., Kissel, J., Krot, A., Langenhorst, F., Lanzirotti, A., Le, L., Leshin, L.A., Leitner, J., Lemelle, L., Leroux, H., Liu, M.-C., Luening, K., Lyon, I., Macpherson, G., Marcus, M.A., Marhas, K., Marty, B., Matrajt, G., Mckeegan, K., Meibom, A., Mennella, V., Messenger, K., Messenger, S., Mikouchi, T., Mostefaoui, S., Nakamura, T., Nakano, T., Newville, M., Nittler, L.R., Ohnishi, I., Ohsumi, K., Okudaira, K., Papanastassiou, D.A., Palma, R., Palumbo, M.E., Pepin, R.O., Perkins, D., Perronnet, M., Pianetta, P., Rao, W., Rietmeijer, F.J.M., Robert, F., Rost, D., Rotundi, A., Ryan, R., Sandford, S.A., Schwandt, C.S., See, T.H., Schlutter, D., Sheffield-Parker, J., Simionovici, A., Simon, S., Sitnitsky, I., Snead, C.J., Spencer, M.K., Stadermann, F.J., Steele, A., Stephan, T., Stroud, R., Susini, J., Sutton, S.R., Suzuki, Y., Taheri, M., Taylor, S., Teslich, N., Tomeoka, K., Tomioka, N., Toppani, A., Trigo-Rodriguez, J.M., Troadec, D., Tsuchiyama, A., Tuzzolino, A.J., Tyliszczak, T., Uesugi, K., Velbel, M., Vellenga, J., Vicenzi, E., Vincze, L., Warren, J., Weber, I., Weisberg, M., Westphal, A.J., Wirick, S., Wooden, D., Wopenka, B., Wozniakiewicz, P., Wright, I., Yabuta, H., Yano, H., Young, E.D., Zare, R.N., Zega, T., Ziegler, K., Zimmerman, L., Zinner, E., Zolensky, M., 2006. Comet 81P/Wild 2 under a microscope. Science 314, 1711–1716.

Busemann, H., Young, A.F., Alexander, C.M.O'D., Hoppe, P., Mukhopadhyay, S., Nittler, L.R., 2006. Interstellar chemistry recorded in organic matter from primitive meteorites. Science 312, 727–730.

Campbell, I.H., Borley, G.D., 1974. The geochemistry of pyroxenes from the lower layered series of the Jimberlana intrusion, Western Australia. Contrib. Mineral. Petrol. 47, 281–297.

Catanzaro, E.J., Murphy, T.J., Garner, E.L., Shields, W.R., 1966. Absolute isotopic abundance ratios and atomic weights of magnesium. J. Res. Natl. Bur. Stand. 70a, 453–458.
Ciesla, F.J., 2007. Outward transport of high-temperature materials around the midplane of the solar nebula. Science 318, 613–615.
Ciesla, F.J., 2010. The distributions and ages of refractory objects in the solar nebula. Icarus 208, 455–467.
Ciesla, F.J., 2011. Residence times of particles in diffusive protoplanetary disk environments. II. Radial motions and applications to dust annealing. Astrophys. J. 740, 9.
Cody, G.D., Heying, E., Alexander, C.M.O., Nittler, L.R., Kilcoyne, A.L.D., Sandford, S.A., Stroud, R.M., 2011. Establishing a molecular relationship between chondritic and cometary organic solids. Proc. Natl. Acad. Sci. USA 108, 19171–19176.
Connelly, J.N., Bizzarro, M., Krot, A.N., Nordlund, Å., Wielandt, D., Ivanova, M.A., 2012. The absolute chronology and thermal processing of solids in the solar protoplanetary disk. Science 338, 651–655.
Connolly Jr., H.C., Huss, G.R., 2010. Compositional evolution of the protoplanetary disk: oxygen isotopes of type-II chondrules from CR2 chondrites. Geochim. Cosmochim. Acta 74, 2473–2483.
Davis, A.M., Richter, F.M., Mendybaev, R.A., Janney, P.E., Wahdwa, M., McKeegan, K.D., 2005. Isotopic mass fractionation laws and the initial Solar System $^{26}Al/^{27}Al$ ratio. Lunar Planet. Sci. XXXVI, 2334.
De Gregorio, B.T., Stroud, R.M., Cody, G.D., Nittler, L.R., Kilcoyne, A.L.D., Wirick, S., 2011. Correlated microanalysis of cometary organic grains returned by Stardust. Meteorit. Planet. Sci. 46, 1376–1396.
Dobrică, E., Brearley, A.J., 2011. Crystalline silicates in comet 81P/Wild 2 from the stardust track 81. Meteorit. Planet. Sci. 46, A59 (abstr.).
Dobrică, E., Engrand, C., Duprat, J., Gounelle, M., Leroux, H., Quirico, E., Rouzaud, J.-N., 2009. Connection between micrometeorites and Wild 2 particles: from Antarctic snow to cometary ices. Meteorit. Planet. Sci. 44, 1643–1661.
Duncan, M.J., Levison, H.F., 1997. A disk of scattered icy objects and the origin of Jupiter-Family comets. Science 276, 1670–1672.
Ebel, D.S., Grossman, L., 2000. Condensation in dust-enriched systems. Geochim. Cosmochim. Acta 64, 339–366.
Elsila, J.E., Galvin, D.P., Dworkin, J.P., 2009. Cometary glycine detected in samples returned by Stardust. Meteorit. Planet. Sci. 44, 1323–1330.
Floss, C., Stadermann, F.J., 2009. High abundances of circumstellar and interstellar C-anomalous phases in the primitive CR3 chondrites QUE 99177 and MET 00426. Astrophys. J. 697, 1242–1255.
Frank, D.R., Zolensky, M.E., Le, L., 2014. Olivine in terminal particles of Stardust aerogel tracks and analogous grains in chondrite matrix. Geochim. Cosmochim. Acta 142, 240–259.
Friedrich, J.M., Ruzicka, A., Rivers, M.L., Ebel, D.S., Thostenson, J.O., Rudolph, R.A., 2013. Metal veins in the Kernouvé (H6 S1) chondrite: evidence for pre- or syn-metamorphic shear deformation. Geochim. Cosmochim. Acta 116, 71–83.
Hughes, A.L.H., Armitage, P.J., 2010. Particle transport in evolving protoplanetary disks: implications for results from Stardust. Astrophys. J. 719, 1633–1653.
Hutcheon, I.D., Marhas, K.K., Krot, A.N., Goswami, J.N., Jones, R.H., 2009. ^{26}Al in plagioclase-rich chondrules in carbonaceous chondrites: evidence for an extended duration of chondrule formation. Geochim. Cosmochim. Acta 73, 5080–5099.
Ishii, H.A., Bradley, J.P., Dai, Z.R., Chi, M., Kearsley, A.T., Burchell, M.J., Browning, N.D., Molster, F., 2008. Comparison of comet 81P/Wild 2 dust with interplanetary dust from comets. Science 319, 447–450.
Ishii, H.A., Joswiak, D., Bradley, J.P., Teslich, N., Matzel, J., Hutcheon, I.D., Brownlee, D., Matrajt, G., MacPherson, G., McKeegan, K.D., 2009. Enabling Al–Mg isotopic measurements on comet Wild 2's Micro-CAIs. Lunar Planet. Sci. XL, 2288.
Ishii, H.A., Stadermann, F.J., Floss, C., Joswiak, D., Bradley, J.P., Teslich, N., Brownlee, D.E., Matrajt, G., MacPherson, G., McKeegan, K.D., 2010. Lack of evidence for in situ decay of aluminum-26 in comet 81P/Wild 2 CAI-like refractory particles 'Inti' and 'Coki'. Lunar Planet. Sci. XLI, 2317.
Joswiak, D.J., Brownlee, D.E., Matrajt, G., Westphal, A.J., Snead, C.J., Gainsforth, Z., 2012. Comprehensive examination of large mineral and rock fragments in Stardust tracks: mineralogy, analogous extraterrestrial materials and source regions. Meteorit. Planet. Sci. 47, 471–524.
Kita, N.T., Ushikubo, T., 2012. Evolution of protoplanetary disk inferred from ^{26}Al chronology of individual chondrules. Meteorit. Planet. Sci. 47, 1108–1119.
Kita, N.T., Nagahara, H., Togashi, S., Morishita, Y., 2000. A short duration of chondrule formation in the solar nebula: evidence from ^{26}Al in Semarkona ferromagnesian chondrules. Geochim. Cosmochim. Acta 64, 3913–3922.
Kita, N.T., Lin, Y., Kimura, M., Morishita, Y., 2004. The ^{26}Al–^{26}Mg chronology of a type C CAI and POIs in Ningqiang carbonaceous chondrite. Lunar Planet. Sci. XXXV, 1471.
Kita, N.T., Ushikubo, T., Fu, B., Valley, J.W., 2009. High precision SIMS oxygen isotope analysis and the effect of sample topography. Chem. Geol. 264, 43–57.
Kita, N.T., Nagahara, H., Tachibana, S., Tomomura, S., Spicuzza, M.J., Fournelle, J.H., Valley, J.W., 2010. High precision SIMS oxygen three isotope study of chondrules in LL3 chondrites: role of ambient gas during chondrule formation. Geochim. Cosmochim. Acta 74, 6610–6635.
Kita, N.T., Ushikubo, T., Knight, K.B., Mendybaev, R.A., Davis, A.M., Richter, F.M., Fournelle, J.H., 2012. Internal ^{26}Al–^{26}Mg isotope systematics of a type B CAI: remelting of refractory precursor solids. Geochim. Cosmochim. Acta 86, 37–51.
Kita, N.T., Yin, Q.-Z., MacPherson, G.J., Ushikubo, T., Jacobsen, B., Nagashima, K., Kurahashi, E., Krot, A.N., Jacobsen, S.B., 2013. ^{26}Al–^{26}Mg isotope systematics of the first solids in the early Solar System. Meteorit. Planet. Sci. 48, 1383–1400.
Krot, A.N., Makide, K., Nagashima, K., Huss, G.R., Ogliore, R.C., Ciesla, F.J., Yang, L., Hellebrand, E., Gaidos, E., 2012. Heterogeneous distribution of ^{26}Al at the birth of the solar system: evidence from refractory grains and inclusions. Meteorit. Planet. Sci. 47, 1948–1979.
Kurahashi, E., Kita, N.T., Nagahara, H., Morishita, Y., 2008a. ^{26}Al–^{26}Mg systematics of chondrules in a primitive CO chondrite. Geochim. Cosmochim. Acta 72, 3865–3883.
Kurahashi, E., Kita, N.T., Nagahara, H., Morishita, Y., 2008b. Al-26–Mg-26 systematics and petrological study of chondrules in CR chondrites. Geochim. Cosmochim. Acta 72, A504 (abstr.).
Larsen, K.K., Triquier, A., Paton, C., Schiller, M., Wielandt, D., Ivanova, M.A., Connelly, J.N., Nordlund, Å., Krot, A.N., Bizzarro, M., 2011. Evidence for magnesium isotope heterogeneity in the solar protoplanetary disk. Astrophys. J. Lett. 735, L37.
Leitner, J., Hoppe, P., Zipfel, J., 2010. First discovery of presolar material of possible supernova origin in impact residues from comet 81P/Wild 2. Lunar Planet. Sci. XLI, 1607.
Leitner, J., Hoppe, P., Zipfel, J., 2012. The C-, N-, and O-isotopic composition of cometary dust from comet 81P/Wild 2. Lunar Planet. Sci. XLIII, 1839.
Ludwig, K.R., 2003. Isoplot 3.00. A geochronological toolkit for Microsoft Excel. In: Berkeley Geochronology Center Special Publication, vol. 4, pp. 1–72.
MacPherson, G.J., Bullock, E.S., Jenny, P.E., Kita, N.T., Ushikubo, T., Davis, A.M., Wadhwa, M., Krot, A.N., 2010. Early solar nebula condensates with canonical, not supracanonical, initial $^{26}Al/^{27}Al$ ratios. Astrophys. J. 711, L117–L121.
MacPherson, G.J., Kita, N.T., Ushikubo, T., Bullock, E.S., Davis, A.M., 2012. Well-resolved variations in the formation ages for Ca–Al-rich inclusions in the early solar system. Earth Planet. Sci. Lett. 331–332, 43–54.
Makide, K., Nagashima, K., Krot, A.N., Huss, G.R., Hutcheon, I.D., Hellebrand, E., Petaev, M.I., 2013. Heterogeneous distribution of ^{26}Al at the birth of the solar system: evidence from corundum-bearing refractory inclusions in carbonaceous chondrites. Geochim. Cosmochim. Acta 110, 190–215.
Maruyama, S., Yurimoto, H., 2003. Relationship among O, Mg isotopes and the petrography of two spinel-bearing compound chondrules. Geochim. Cosmochim. Acta 67, 3943–3957.
Matrajt, G., Ito, M., Wirick, S., Messenger, S., Brownlee, D.E., Joswiak, D.J., Flynn, G., Sandford, S., Snead, C., Westphal, A., 2008. Carbon investigation of two Stardust particles: a TEM, NanoSIMS, and XANES study. Meteorit. Planet. Sci. 43, 315–334.
Matzel, J.E.P., Ishii, H.A., Joswiak, D., Hutcheon, I.D., Bradley, J.P., Brownlee, D., Weber, P.K., Teslich, N., Matrajt, G., McKeegan, K.D., MacPherson, G.J., 2010. Constraints on the formation age of cometary material from the NASA stardust mission. Science 328, 483–486.
McKeegan, K.D., Aléon, J., Bradley, J., Brownlee, D., Busemann, H., Butterworth, A., Chaussidon, M., Fallon, S., Floss, C., Gilmour, J., Gounelle, M., Graham, G., Guan, Y., Heck, P.R., Hoppe, P., Hutcheon, I.D., Huth, J., Ishii, H., Ito, M., Jacobsen, S.B., Kearsley, A., Leshin, L.A., Liu, M.-C., Lyon, I., Marhas, K., Marty, B., Matrajt, G., Meibom, A., Messenger, S., Mostefaoui, S., Mukhopadhyay, S., Nakamura-Messenger, K., Nittler, L., Palma, R., Pepin, R.O., Papanastassiou, D.A., Robert, F., Schlutter, D., Snead, C.J., Stadermann, F.J., Stroud, R., Tsou, P., Westphal, A., Young, E.D., Ziegler, K., Zimmermann, L., Zinner, E., 2006. Isotopic compositions of cometary matter returned by Stardust. Science 314, 1724–1728.
Messenger, S., Joswiak, D.J., Ito, M., Matrajt, G., Brownlee, D.E., 2009. Discovery of presolar SiC from comet Wild-2. Lunar Planet. Sci. XL, 1790.
Mikouchi, T., Tachikawa, O., Hagiya, K., Ohsumi, K., Suzuki, Y., Uesugi, K., Takeuchi, A., Zolensky, M.E., 2007. Mineralogy and crystallography of comet 81P/Wild 2 particles. Lunar Planet. Sci. XXXVIII, 1946.
Mittlefehldt, D.W., McCoy, T.J., Goodrich, C.A., Kracher, A., 1998. Non-chondritic meteorites from asteroidal bodies. In: Papike, J.J. (Ed.), Planetary Materials. In: Rev. Mineral., vol. 36. Mineralogical Society of America, Washington, DC, pp. 4-1–4-195.
Nagashima, K., Krot, A.N., Chaussidon, M., 2007. Aluminum–magnesium isotope systematics of chondrules from CR chondrites. Meteorit. Planet. Sci. 42, A115 (abstr.).
Nagashima, K., Krot, A.N., Huss, G.R., 2008. ^{26}Al in chondrules from CR carbonaceous chondrites. Lunar Planet. Sci. XXXIX, 2224.
Nakamura, T., Noguchi, T., Tsuchiyama, A., Ushikubo, T., Kita, N.T., Valley, J.W., Zolensky, M.E., Kakazu, Y., Sakamoto, K., Mashio, E., Uesugi, K., Nakano, T., 2008. Chondrulelike objects in short-period comet 81P/Wild 2. Science 321, 1664–1667.
Nakamura, T., Noguchi, T., Tsuchiyama, A., Ushikubo, T., Kita, N.T., Valley, J.W., Takahata, N., Sano, Y., Zolensky, M.E., Kakazu, Y., Uesugi, K., Nakano, T., 2009. Additional evidence for the presence of chondrules in Comet 81P/Wild 2. Meteorit. Planet. Sci. 44, A153 (abstr.).
Nakashima, D., Kimura, M., Yamada, K., Noguchi, T., Ushikubo, T., Kita, N.T., 2010. Study of chondrules in CH chondrites – I: oxygen isotope ratios of chondrules. Meteorit. Planet. Sci. 45, A148 (abstr.).

Nakashima, D., Ushikubo, T., Rudraswami, N.G., Kita, N.T., Valley, J.W., Nagao, K., 2011a. Ion microprobe analyses of oxygen three-isotope ratios of chondrules from the Sayh al Uhaymir 290 chondrite using a multiple-hole disk. Meteorit. Planet. Sci. 46, 857–874.

Nakashima, D., Ushikubo, T., Zolensky, M.E., Weisberg, M.K., Joswiak, D.J., Brownlee, D.E., Matrajt, G., Kita, N.T., 2011b. High precision oxygen three isotope analysis of Wild 2 particles and anhydrous chondritic interplanetary dust particles. Lunar Planet. Sci. XLII, 1240.

Nakashima, D., Ushikubo, T., Joswiak, D.J., Brownlee, D.E., Matrajt, G., Weisberg, M.K., Zolensky, M.E., Kita, N.T., 2012. Oxygen isotopes in crystalline silicates of comet Wild 2: a comparison of oxygen isotope systematics between Wild 2 particles and chondritic materials. Earth Planet. Sci. Lett. 357–358, 355–365.

Norris, T.L., Gancarz, A.J., Rokop, D.J., Thomas, K.W., 1983. Half-life of ^{26}Al. J. Geophys. Res. 88, B331–B333.

Ogliore, R.C., Huss, G.R., Nagashima, K., Butterworth, A.L., Gainsforth, Z., Stodolna, J., Westphal, A.J., Joswiak, D., Tyliszczak, T., 2012. Incorporation of a late-forming chondrule into comet Wild 2. Astrophys. J. 745, L19.

Richter, F.M., Janney, P.E., Mendybaev, R.A., Davis, A.M., Wadhwa, M., 2007. Elemental and isotopic fractionation of Type B CAI-like liquids by evaporation. Geochim. Cosmochim. Acta 71, 5544–5564.

Sahijpal, S., Goswami, J.N., 1998. Refractory phases in primitive meteorites devoid of ^{26}Al and ^{41}Ca: representative samples of first solar system solids? Astrophys. J. 509, L137–L140.

Sandford, S.A., 2008. Terrestrial analysis of the organic component of comet dust. Annu. Rev. Anal. Chem. 1, 549–578.

Sandford, S.A., Aléon, J., Alexander, C.M.O., Araki, T., Bajt, S., Baratta, G.A., Borg, J., Bradley, J.P., Brownlee, D.E., Brucato, J.R., Burchell, M.J., Busemann, H., Butterworth, A., Clemett, S.J., Cody, G., Colangeli, L., Cooper, G., D'Hendecourt, L., Djouadi, Z., Dworkin, J.P., Ferrini, G., Fleckenstein, H., Flynn, G.J., Franchi, I.A., Fries, M., Gilles, M.K., Glavin, D.P., Gounelle, M., Grossemy, F., Jacobsen, C., Keller, L.P., Kilcoyne, A.L.D., Leitner, J., Matrajt, G., Meibom, A., Mennella, V., Mostefaoui, S., Nittler, L.R., Palumbo, M.E., Papanastassiou, D.A., Robert, F., Rotundi, A., Snead, C.J., Spencer, M.K., Stadermann, F.J., Steele, A., Stephan, T., Tsou, P., Tyliszczak, T., Westphal, A.J., Wirick, S., Wopenka, B., Yabuta, H., Zare, R.N., Zolensky, M.E., 2006. Organics captured from comet 81P/Wild 2 by the Stardust Spacecraft. Science 314, 1720–1724.

Schrader, D.L., Connolly Jr., H.C., Lauretta, D.S., Nagashima, K., Huss, G.R., Davidson, J., Domanik, K.J., 2013a. The formation and alteration of the Renazzo-like carbonaceous chondrites II: linking O-isotope composition and oxidation state of chondrule olivine. Geochim. Cosmochim. Acta 101, 302–327.

Schrader, D.L., Nagashima, K., Krot, A.N., Ogliore, R.C., Yin, Q.-Z., Amelin, Y., 2013b. Testing the distribution of ^{26}Al in the protoplanetary disk using CR chondrules. Meteorit. Planet. Sci. 48, 5141 (abstr.).

Schrader, D.L., Nagashima, K., Krot, A.N., Ogliore, R.C., Hellebrand, E., 2014. Variations in the O-isotope composition of gas during the formation of chondrules from the CR chondrites. Geochim. Cosmochim. Acta 132, 50–74.

Simon, S.B., Joswiak, D.J., Ishii, H.A., Bradley, J.P., Chi, M., Grossman, L., Aléon, J., Brownlee, D.E., Fallon, S., Hutcheon, I.D., Matrajt, G., McKeegan, K.D., 2008. A refractory inclusion returned by Stardust from comet 81P/Wild 2. Meteorit. Planet. Sci. 43, 1861–1877.

Slodzian, G., Hillion, F., Stadermann, F.J., Zinner, E., 2004. QSA influences on isotopic ratio measurements. Appl. Surf. Sci. 231–232, 874–877.

Stadermann, F.J., Hoppe, P., Floss, C., Heck, P.R., Horz, F., Huth, J., Kearsley, A.T., Leitner, J., Marhas, K.K., McKeegan, K.D., Stephan, T., 2008. Stardust in Stardust – the C, N, and O isotopic compositions of Wild 2 cometary matter in Al foil impacts. Meteorit. Planet. Sci. 43, 299–313.

Tenner, T.J., Ushikubo, T., Kurahashi, E., Nagahara, H., Kita, N.T., 2013a. Oxygen isotope systematics of chondrule phenocrysts from the CO3.0 chondrite Yamato 81020: evidence for two distinct oxygen isotope reservoirs. Geochim. Cosmochim. Acta 102, 226–245.

Tenner, T.J., Ushikubo, T., Nakashima, D., Kita, N.T., Weisberg, M.K., 2013b. ^{26}Al in chondrules from the CR3.0 chondrite Queen Alexandra Range 99177: a link with O isotopes. Lunar Planet. Sci. XLIV, 2010.

Tenner, T.J., Nakashima, D., Ushikubo, T., Kita, N.T., Weisberg, M.K., in press. Oxygen isotope ratios of FeO-poor chondrules in CR3 chondrites: influence of dust enrichment and H_2O during chondrule formation. Geochim. Cosmochim. Acta. http://dx.doi.org/10.1016/j.gca.2014.09.025.

Tenner, T.J., Ushikubo, T., Nakashima, D., Kita, N.T., Weisberg, M.K., Kimura, M., 2014b. Silica excess in anorthitic plagioclase from type 3.00 chondrite chondrules: Evidence for retaining primary ^{26}Al–^{26}Mg systematics. Lunar Planet. Sci. XLV, 1187.

Ushikubo, T., Kimura, M., Kita, N.T., Valley, J.W., 2012. Primordial oxygen isotope reservoirs of the solar nebula recorded in chondrules in Acfer 094 carbonaceous chondrite. Geochim. Cosmochim. Acta 90, 242–264.

Ushikubo, T., Nakashima, D., Kimura, M., Tenner, T.J., Kita, N.T., 2013. Contemporaneous formation of chondrules in distinct oxygen isotope reservoirs. Geochim. Cosmochim. Acta 109, 280–295.

Van Orman, J.A., Cherniak, D.J., Kita, N.T., 2014. Magnesium diffusion in plagioclase: dependence on composition, and implications for thermal resetting of the ^{26}Al–^{26}Mg early solar system chronometer. Earth Planet. Sci. Lett. 385, 79–88.

Weisberg, M.K., Prinz, M., Clayton, R.N., Mayeda, T.K., Grady, M.M., Pillinger, C.T., 1995. The CR chondrite clan. In: Proc. NIPR Symp. Antarct. Meteorites, vol. 8, pp. 11–32.

Weisberg, M.K., Ebel, D.S., Connolly Jr., H.C., Kita, N.T., Ushikubo, T., 2011. Petrology and oxygen isotope compositions of chondrules in E3 chondrites. Geochim. Cosmochim. Acta 75, 6556–6569.

Zolensky, M.E., Zega, T.J., Yano, H., Wirick, S., Westphal, A.J., Weisberg, M.K., Weber, I., Warren, J.L., Velbel, M.A., Tsuchiyama, A., Tsou, P., Toppani, A., Tomioka, N., Tomeoka, K., Teslich, N., Taheri, M., Susini, J., Stroud, R., Stephan, T., Stadermann, F.J., Snead, C.J., Simon, S.B., Simionovici, A., See, T.H., Robert, F., Rietmeijer, F.J.M., Rao, W., Perronnet, M.C., Papanastassiou, D.A., Okudaira, K., Ohsumi, K., Ohnishi, I., Nakamura-Messenger, K., Nakamura, T., Mostefaoui, S., Mikouchi, T., Meibom, A., Matrajt, G., Marcus, M.A., Leroux, H., Lemelle, L., Le, L., Lanzirotti, A., Langenhorst, F., Krot, A.N., Keller, L.P., Kearsley, A.T., Joswiak, D., Jacob, D., Ishii, H., Harvey, R., Hagiya, K., Grossman, L., Grossman, J.N., Graham, G.A., Gounelle, M., Gillet, P., Genge, M.J., Flynn, G., Ferroir, T., Fallon, S., Ebel, D.S., Dai, Z.R., Cordier, P., Clark, B., Chi, M., Butterworth, A.L., Brownlee, D.E., Bridges, J.C., Brennan, S., Brearley, A., Bradley, J.P., Bleuet, P., Bland, P.A., Bastien, R., 2006. Mineralogy and petrology of Comet 81P/Wild 2 nucleus samples. Science 314, 1735–1739.